**Proceedings of
the ASME Conference on Smart Materials,
Adaptive Structures & Intelligent Systems
Sept. 21 – 23, 2015, Colorado Springs, CO, USA**

SMASIS2015-8895

FUSED FILAMENT ADDITIVE MANUFACTURING OF IONIC POLYMER-METAL COMPOSITE SOFT ACTIVE 3D STRUCTURES

James D. Carrico[a], Nicklaus W. Traeden[a], Matteo Aureli[b] and Kam K. Leang[a*]
[a]Design, Automation, Robotics, & Control (DARC) Lab, Dept. of Mech. Engineering, Univ. of Utah, Salt Lake City, UT
[b]Multiphysics Laboratory, Dept. of Mech. Engineering, Univ. of Nevada Reno, Reno, NV

ABSTRACT

*This paper describes a new three-dimensional (3D) additive manufacturing (AM) technique in which electroactive polymer filament material is used to build soft active 3D structures, layer by layer. The proposed manufacturing process is well-suited for creating electroactive soft complex structures and devices, whereby the entire system can be manufactured from an electroactive polymer material. For the first time, the unique actuation and sensing properties of ionic polymer-metal composite (IPMC) is exploited and directly incorporated into the structural design to create sub-millimeter scale cilia-like actuators and sensors to macro-scale soft robotic systems. Because ionic polymers such as Nafion are not melt-processable, in the first step a precursor material (non-acid Nafion precursor resin) is extruded into a thermoplastic filament for 3D printing. The filament is then used by a custom-designed 3D printer to manufacture the desired soft polymer structures, layer by layer. Since, at this stage the 3D-printed samples are not yet electroactive, a chemical functionalization process follows, consisting in hydrolyzing the precursor resin in an aqueous solution of sodium hydroxide (*NaOH*) and dimethyl sulfoxide (DMSO,* C_2H_6OS*). Upon functionalization, metal electrodes are applied on the samples through an electroless plating process, which enables selected areas of the 3D-printed electroactive structures to be controlled by voltage signals for actuation, while other parts can function as sensors. This innovative AM process is described in detail and experimental results are presented to demonstrate the potential and feasibility of creating 3D-printed IPMC actuator samples.*

1 Introduction

Fused filament additive manufacturing (AM), such as three-dimensional (3D) printing, is a manufacturing technique in which materials such as plastic or metal are deposited in layers to produce a 3D structure, often times with complex shapes and features [1]. Non-electroactive plastics such as acrylonitrile butadiene styrene (ABS) and polylactic acid (PLA) are typically used to create components in applications ranging from medical devices to robotics [2]. In contrast, presented here is a novel fused filament AM technique using electroactive ionomeric polymer material to create 3D soft ionic polymer-metal composite (IPMC) electroactive structures for applications such as soft robotics and novel biomedical devices.

The proposed novel manufacturing paradigm is illustrated in Fig. 1. First, a solid model of a soft active structure, for example the body of a soft robotic system, is created in a computer aided design (CAD) software package as illustrated in Fig. 1(a). Ideally, the body would be a monolithic structure designed with certain sections having actuation capabilities and others with sensing capabilities. Next, the solid model is sent to a custom-designed 3D printer that utilizes an ionomeric precursor filament material to manufacture the fused filament soft polymer structure, layer by layer, as shown in Fig. 1(b). The manufactured component is then chemically "activated" and plated with electrodes as shown in Fig. 1(c), to create a fully electroactive body. Finally, electronics and a power source can be added to the manufactured structure to create the complete robotic system with built-in actuation and sensing capabilities, as shown in Fig. 1(d).

Ionic polymer-metal composites consist of an ion exchange membrane (such as the perfluorosulfonic polymer, Nafion) sandwiched between two noble metal (typically platinum) electrodes [3–5]. When the IPMC is hydrated with a solvent, such as water, application of an electric potential causes the cations to move toward the cathode, dragging along with them water molecules. Water accumulation at the cathode side causes differential "swelling" in the ionomeric material and, therefore, macroscopic bending. As a result, the electromechanical response of the IPMC material allows it to function as an actuator. Conversely, if the IPMC is deformed, the cations redis-

*Corresponding author; Email: kam.k.leang@utah.edu.

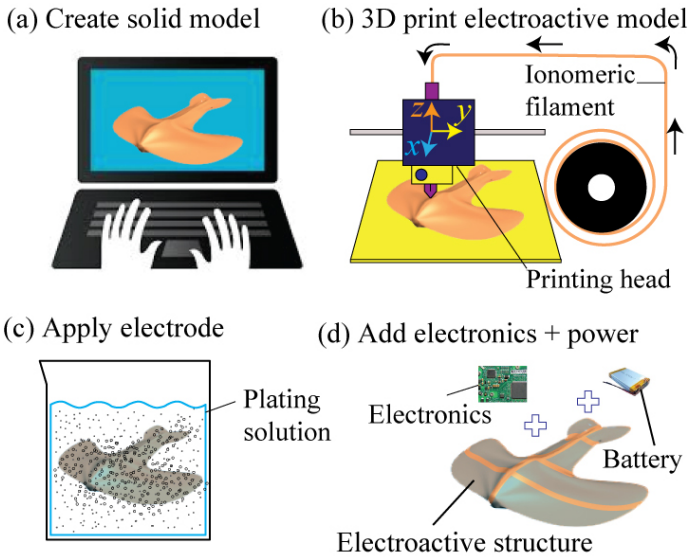

Figure 1. Ionomeric filament 3D printing to create IPMC-based soft active structure: (a) Device designed using computer aided design (CAD) software. (b) Model is sent to a 3D printer that uses ionomeric filament material for 3D printing. (c) The body is "activated" and electrodes are applied using an electroless plating procedure. (d) Finally, electronics and a power source are added to create a monolithic soft robotic system.

tribute and create a voltage signal across the electrodes [3, 5]. Thus, IPMCs can also be used as sensors. Some of the advantages of IPMCs include low actuation voltage (<5 V), flexibility, softness, and that they are easy to shape. Therefore, IPMCs are attractive for use in a wide variety of soft active systems, including active catheters [6, 7], physical sensors [8], micro pumps [9–12], and propulsion mechanisms for underwater robotics [13–15]. Currently, the most popular approach to create IPMC actuators and sensors is by using commercially available Nafion sheets or tubes. Fabrication techniques such as hot pressing or solution casting are also employed to create custom-shaped IPMCs [16,17]. Herein, the AM technique is exploited to quickly and efficiently create custom 3D IPMC soft active structures for applications such as soft robotics.

Soft active structures and robots are attractive in general, because soft structures are less likely to cause damage to sensitive systems [18], they can be used to create novel dexterous grippers [19] as well as durable and versatile sensors [20] and can easily achieve complex modes of actuation with only a single actuated degree of freedom [21]. Soft active structures and robots have been manufactured via nano-imprint methods, laser imaging, laser ablation, micro injection molding, embedded molding and, recently soft material deposition processes like 3D printing [22, 23]. However, subsequent to these processes separately manufactured actuators such as thermally activated joints [24], shape memory alloys [25] or piezoelectric fibers [26] have had to be embedded in the soft structure [23]. Thus, the manufacturing of such soft complex devices involves fabricating a soft passive structure and then attaching and/or embedding actuators (such as DC motors or pneumatics) and sensors (such as strain gages) for motion control and sensing [23].

Instead, the proposed additive manufacturing technique that utilizes precursor polymer enables rapid manufacturing of soft electroactive structures with integrated actuators and sensors. Thus, the manufacturing process is simplified and actuators and sensors are more easily incorporated into the 3D structure. The contributions of this paper are a detailed description of the IPMC 3D printing technique and a demonstration of a working 3D printed IPMC actuator sample.

The remainder of this paper is organized as follows. Section 2 discusses the 3D printing process, beginning with an overview of conventional IPMC fabrication techniques and their limitations. Afterwards, experimental results for 3D printed samples are discussed in Section 3. Finally, concluding remarks and a discussion of future work are presented in Section 4.

2 IPMC 3D Printing Process

This section focuses on the details of the AM (3D printing) technique for IPMC materials. The section begins with a summary of state-of-the-art manufacturing processes for IPMCs and their limitations. Then, the extrusion of the precursor filament for use in the 3D printing process is discussed. Finally, this section describes the 3D printer design and the 3D printing process tuning.

2.1 IPMC Manufacturing: State-of-the-Art

Conventional means of fabricating IPMCs consist of shaping and plating commercially available sheets or tubular structures from Nafion or other ion exchange membranes. Thus, existing IPMC actuators and sensors come in limited shapes, primarily thin sheet-like structures. To overcome this limitation, researchers have created other shapes either by fusing multiple membranes together via a hot pressing method [16] to create thicker structures or by dispensing dispersions of Nafion into a cast [17]. But these methods only produce predefined shapes and are time-consuming. Free-form layer-by-layer manufacturing of IPMCs is described in [27] and [28], where that initial work was based on dispensing layers of Nafion dispersions into silicone casts and allowing the solvent in the dispersion to evaporate away. This dispersion based method allowed for creation of the electrode layer as well as the ionomeric substrate by dispensing first layers of dispersion with electrode particles in them and then printing these same layers at the end. However, there were several challenges encountered implementing this fabrication technique, namely, requiring a plasticizer, requiring extensive drying time and the resulting IPMCs were observed to have significantly lower blocking force than conventionally manufactured IPMCs [27]. By exploiting the fused filament additive manufacturing (3D printing) technique it is possible to manufacture IPMCs of almost any shape, at a faster rate, with a more accessible technology.

The fabrication technique described here begins with extruding Nafion filament from commercially obtained Nafion R1100 precursor polymer using a custom designed filament extruder. Then, the filament is used in a custom-designed 3D printer to create 3D-printed IPMC samples. The samples are then hydrolyzed to "activate" them and subsequently electrodes are

applied through an electroless plating process. In the future, the overall processing time can potentially be significantly improved by developing "activation" and plating processes integrated within the printing process. This is especially pertinent to the hydrolysis process, the duration of which depends on the thickness of the precursor material it is being applied to. By integrating the hydrolysis process into the printing process, individual layers of precursor material could be hydrolyzed immediately after they are printed.

2.2 Filament Extruder Design

Nafion is the most commonly used material in IPMCs [3, 5]. Nafion consists of a hydrophobic tetrafluoroethylene (Teflon) backbone and hydrophilic perfluorovinyl ether side chains, with sulfonate end groups [29]. When hydrated, a network of hydrophilic regions is formed and the sulfonate end groups of the side chains disassociate from their cations. Those cations then constitute free charges which are able to migrate through the hydrophilic network, giving Nafion its characteristic conductivity [29]. Unfortunately, the ionic end groups that are responsible for this characteristic functionality of "active" Nafion, also prevents it from being melt processable [30]. Therefore, in order to extrude, print or otherwise melt-process Nafion, it is necessary to obtain Nafion in its sulfonyl fluoride precursor form which, in contrast, is melt processable. Thus, after the precursor polymer is formed into its desired geometry it has to be "activated" via a hydrolysis process that converts the sulfonyl end groups to sulfonic acid or salt. The "active" Nafion can then be plated using any effective plating procedure to create functional IPMCs [5, 31–33].

An extruder was designed and built to produce Nafion precursor filament for the custom-designed 3D printer. The extruder is shown in Fig. 2 and it consists of a hopper loaded with pellets of the Nafion precursor polymer, and a single screw drive auger (5/8-inch diameter, 0.66 threads per inch, single fluted) coupled to a 24 volt DC motor (with a 1:144 gear ratio) that feeds the raw polymer through a conduit to a heated nozzle. The nozzle tapers down to the nominal desired filament diameter, 1.75 mm. Down stream of the extruder, the filament is drawn by a pair of rollers driven by another DC motor.

The extrusion of the filament occurs at a temperature between 280°C and 300°C. Extrusion speed varies from 25-125 mm/s depending on temperature, motor voltage (between 10 and 24 volts), and the amount of material in the auger.

2.3 3D Printer Design and Tuning

A custom designed 3D printer was fabricated based on the commercially available Mendel RepRap 3D printer. As shown in Fig. 3(a), the printer consists of a two degree-of-freedom printing head, and a one degree-of-freedom heated build stage. The printing head system is custom designed to accommodate the high melting temperature of the Nafion precursor and the flexible nature of the precursor filament. This system, shown in Fig. 3(b) and (c), is comprised of a heated nozzle, a filament drive mechanism, and a thermal barrier. The heated nozzle uses a high power flame-proof resistor to reach temperatures in excess of 300 °C. A thermistor is attached to the heated nozzle to relay the temperature measurement back to the printer electronics and computer for displaying the temperature. An external thermocouple temperature sensor was also attached to the heated nozzle to monitor and verify the temperature.

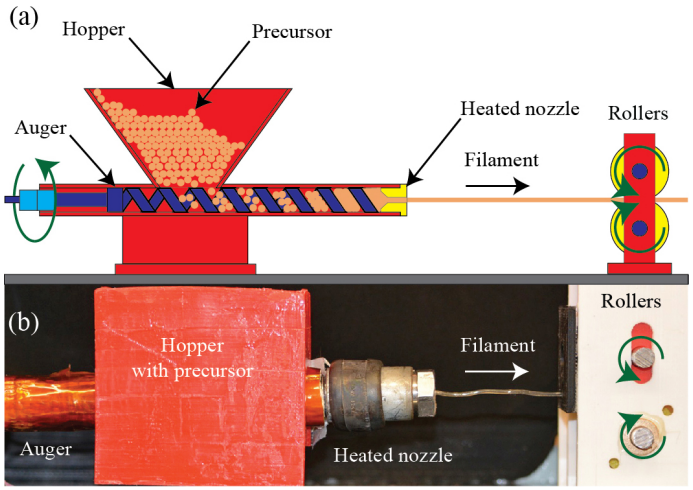

Figure 2. Nafion precursor filament extruder: (a) diagram of main components such as an auger, a hopper, a heated nozzle, and rollers. (b) Photograph of custom-designed extruder.

The filament drive mechanism is responsible for pushing the filament through the heated nozzle onto the build platform. This is accomplished via a bearing that pushes the filament into a toothed feed gear that is directly driven by a high torque stepper motor. The flexible nature of the precursor material requires the path of the filament between the filament driver and the nozzle to be highly constrained to prevent buckling of the filament. In addition, the transition region between the solid and melted precursor material is designed to be very small. This keeps the frictional forces of the filament against the inside of the barrel to a minimum and is accomplished by a custom designed thermal barrier between the filament drive and the heated nozzle. The back-pressure on the filament is highly sensitive to the diameter of the nozzle opening.

The heated build stage can sustain temperatures above 200°C. The Nafion precursor material is "printed" onto the build stage by controlling the motion of the printing head and the build stage as the precursor material is extruded. Pronterface software is used to control the printer. That software uses gcode generated from Slic3r software, which slices stl-CAD models that are produced in Solidworks CAD program. The effective settings for printing Nafion precursor material were found to be a bed temperature of approximately 180 °C, a nozzle temperature of 290 °C. The feedrate of the printer is limited by filament buckling dependent on the available torque of the feed motor and size of the nozzle opening. Faster speeds are possible with higher torque and a larger nozzle diameter with a loss in print resolution. In this application prints were made with a 0.5mm nozzle at a rate of 15mm/s.

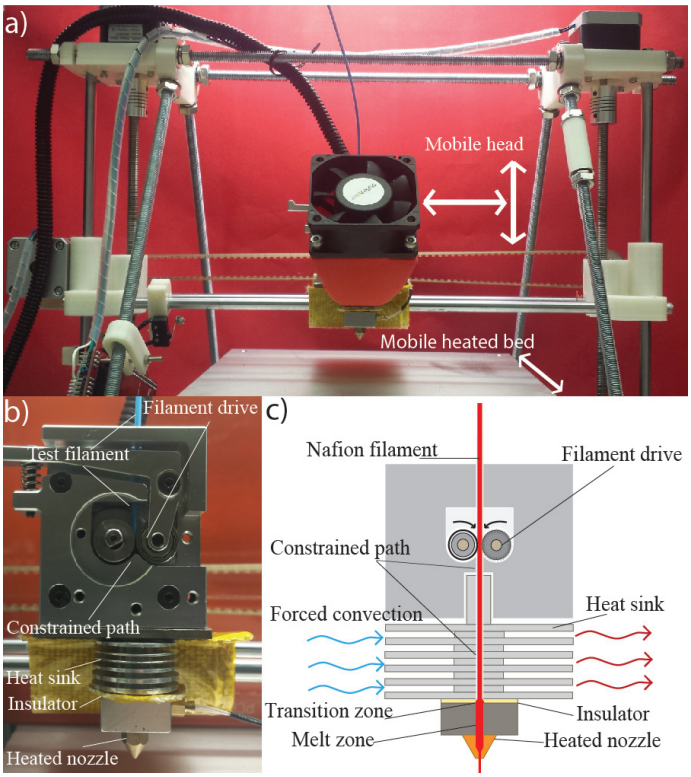

Figure 3. Custom-designed Nafion fused filament three dimensional printer: (a) Photo of the custom Nafion printer assembly, (b) Photo of the printer head and (c) Illustration of the printer head showing the main components.

2.4 Activation Process

As illustrated in Fig. 4(a), the activation process involves hydrolyzing the Nafion precursor in a solution of 15 wt% KOH / 35 wt% DMSO / 50 wt% deionized water at 75°C as prescribed by the manufacturer [34]. The material is then cleaned by soaking it in three successive baths of deionized water at 75°C for 30 minutes each. Figure 4(b) shows how fluorine atoms on the sulfonyl end groups are exchanged with hydroxide from the solution and how the hydrogen ion from this hydroxide group is then exchanged with the potassium ion resulting in the potassium salt form, in the hydrolysis process [35]. This process proceeds from the surface of the polymer inward, as the hydrolysis of exterior layers allows the swelling of the membrane. Assuming a hydrolysis rate of approximately 1.3 μm per minute, a 0.5-mm thick sample would soak for 4 hours to complete the hydrolysis and then for another 4 hours to allow for the formation of ionic clusters throughout the material [35]. The complete hydrolysis of the sample can be confirmed after approximately 4 hours by the complete staining of a cross-section of the sample using methylene blue, which will only die the "activated" material [35].

2.5 Electrode Plating Process

The electroless plating process used here is similar to that reported in [31] and [33]. The electroless plating of the Nafion membranes with platinum electrodes is divided into four distinct processes: (1) the surface preparation, cleaning and initial ion

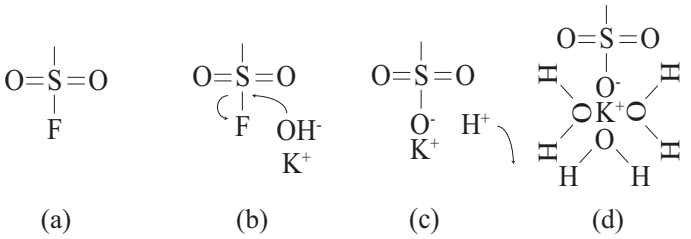

Figure 4. Activation of Nafion precursor material: (a) End groups of the precursor side chains in their sulfonyl fluoride form. (b) Fluorine atoms on the sulfonyl end groups are electrophilicly exchanged with hydroxyl ions. (c) The hydrogen ions in the hydroxyl group is nucleophilicly exchanged with the potassium ions. (d) A hydration sphere forms around the potassium ion, swelling the hydrolyzed material [35].

exchange process, (2) the primary plating process, (3) the secondary plating process, and (4) a final ion exchange process. Some processes are repeated multiple times. For instance, the secondary plating process is repeated until the resistance across the electrode surfaces is less than 5 Ω/cm. There are cleaning steps at the end of the two plating processes to prevent contamination of subsequent processes. All processes are conducted in a fume hood due to the toxicity of the chemicals involved. The details of each process are illustrated in Fig. 5 and listed below.

1. *Surface preparation, cleaning, and initial ion exchange process:* With conventional Nafion membranes, the first step is to roughen the membrane with 200 grit sandpaper (where roughening is done in the direction of the intended bending axis), to increase the surface area of the interface between the Nafion and the electrode material. This was not done to the printed samples to avoid damaging them and because it was presumed that the printed surface would not be as smooth as a conventional ion-exchange membrane. Next, the samples are soaked in deionized (DI) water at 65°C for 15 minutes to swell them, if they are dry. Then, the samples are soaked in 3 wt% H_2O_2 at 65°C for 45 minutes. Next, the samples are soaked in deionized (DI) water at 65°C for 15 minutes. Then the samples are soaked in 15 wt%. H_2SO_4 at 65°C for 45 minutes to clean the membrane and convert it to its acid form. In this step, the potassium ion from hydrolysis is replaced by a hydrogen ion. This is done to facilitate subsequent ion exchanges. The samples are then soaked in two more successive baths of (DI) water at 65°C for 45 minutes.
2. *Primary plating process:* The samples of active Nafion are soaked in a 0.02 molar solution of Tetraammineplatinum(II) chloride hydrate ($Pt(NH_3)_4Cl_2$) for 3 to 4 hours at room temperature. This accomplishes an ion exchange in the surface layers of the membrane in which the Pt^+ ion replaces the H^+ ion. The membrane is then immersed in deionized water at 50°C, to which a reducing agent ($NaBH_4$) is added every 30 minutes for three hours while slowly raising the temperature to 65°C. This visibly metalizes the surface layers of the membrane. Afterwards, the sample is soaked in 0.5 M H_2SO_4 at 65°C for 45 minutes, followed by soaking the samples in two successive baths of DI water at 65°C for 45 minutes to clean it. This process is repeated once.

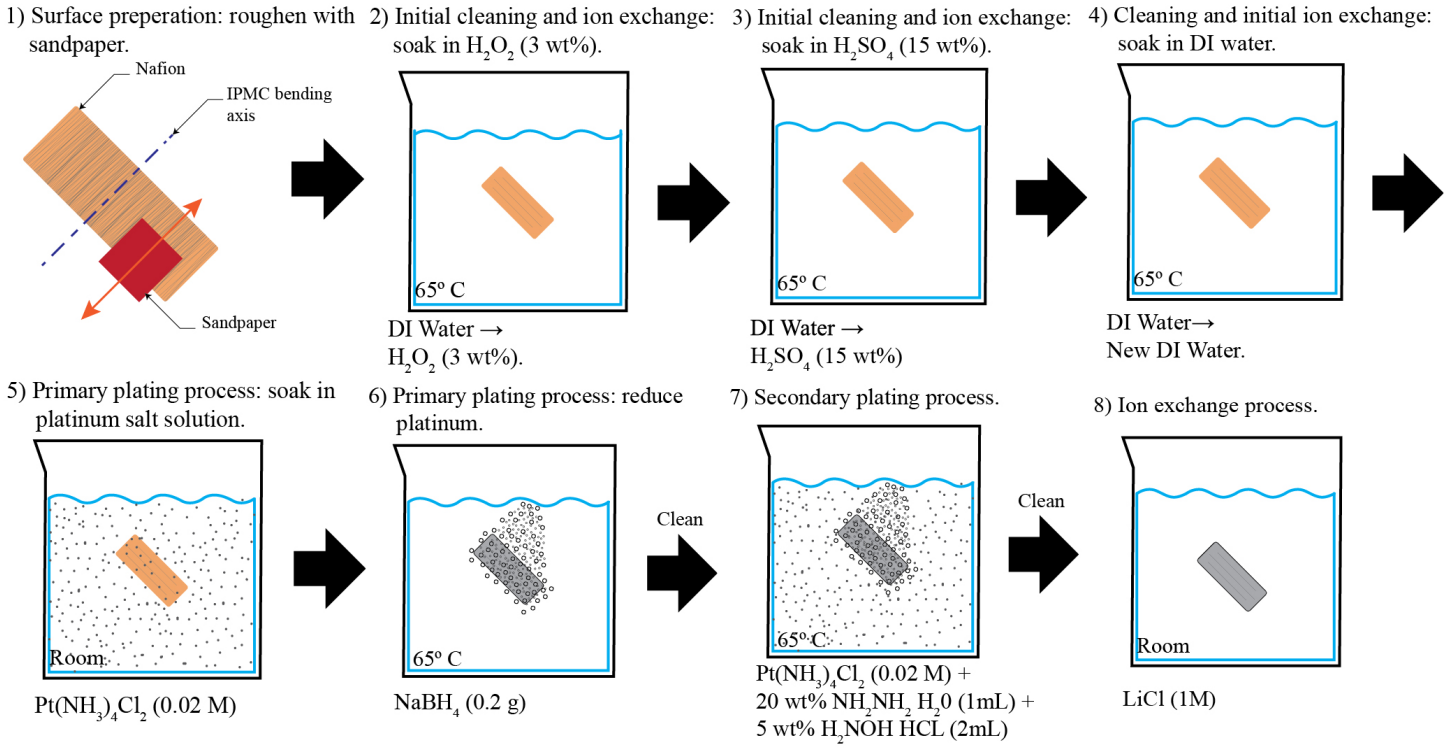

Figure 5. The electroless plating process: Arrows with the word "clean" over them indicate an intermediate process of soaking the sample in 0.5 M H_2SO_4 at 65°C for 45 minutes, followed by soaking the sample in two successive baths of DI water at 65°C for 45 minutes.

3. *Secondary plating process:* The samples of active Nafion are again immersed in Tetraammineplatinum(II) chloride hydrate ($Pt(NH_3)_4Cl_2$) at 50°C. However, reducing agents (5 wt% hydroxylamine hydrochloride and 20 wt% hydrazine) are this time added directly to the platinum salt solution, every 30 minutes, while slowly raising the temperature to 65°C over the coarse of 3 hours. This causes platinum to be deposited on the surface of the existing metalized layers, improving the electrical conductivity of these layers. Then the resistance of the electrodes are measured and if they are above 10 Ω the process is repeated. Afterwards, the sample is soaked in 0.5 M H_2SO_4 at 65°C for 45 minutes, followed by soaking the samples in two successive baths of DI water at 65°C for 45 minutes to clean it.
4. *Ion exchange process:* The ion exchange process is done by soaking the membrane in a 1 molar LiCl solution at room temperature for 24 hours. This converts the fabricated IPMCs into their lithium salt form, improving their actuation characteristics [32].

3 Experimental Results and Discussion

This section describes the experimental results, including the extruded filament, the 3D printed samples, and experimental verification of the functionality of 3D printed IPMC samples.

3.1 Extruded Nafion Filament

The extrusion of the Nafion filament was conducted between 280°C and 300°C. It was found that it was effective to draw the material at a slightly lower speed than it was being extruded, to prevent significant necking. The extrusion was conducted in a fume hood due to the potential for the production of hydrogen fluoride (HF) and other toxic gases when Nafion precursor is heated.

Examples of the Nafion filament obtained are shown in Fig. 6. The discoloration in the filament on the right is attributed to contamination possibly caused by accelerated oxidation of the extruder components. This would be the result of the release of trace amounts of HF during the extrusion process. This discoloration dissipated during the printing process and subsequent chemical treatments. The filament obtained was soft and flexible and had a Teflon-like texture. The resulting diameter of the extruded Nafion filament was 1.75 mm ±0.1 mm. The 3D printer nozzle and filament feed mechanism were designed to accommodate this filament diameter.

3.2 Printed Samples

Membranes of the Nafion precursor material printed by the 3D printer are shown in Fig. 7(a1). The samples are approximately 5 mm × 10 mm with a thickness of 0.5-mm. As shown in Fig. 7(b1), these membranes were then made into IPMCs by using the electroless plating process described previously. For the sake of comparison, IPMCs made from membranes cut from commercially obtained 0.5 mm thick Nafion sheet, plated using the same electroless plating process are also shown. The commercially obtained membranes are shown in Fig. 7(a2) and the resulting IPMCs are shown in Fig. 7(b2). The printed Nafion membranes are more textured than the membranes cut from com-

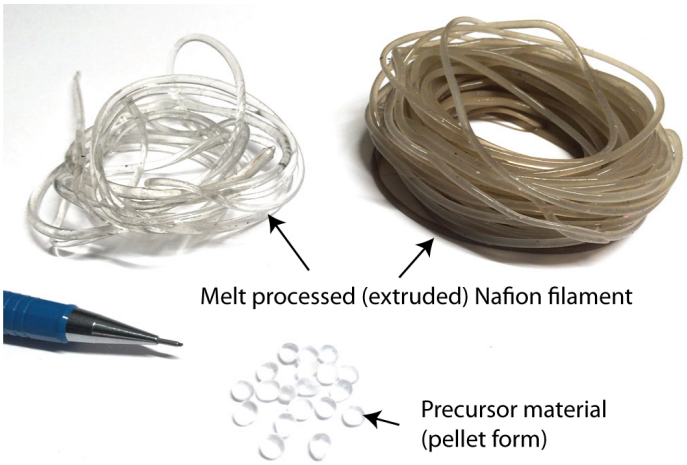

Figure 6. Samples of Nafion precursor filament obtained from extruding it as described. Discoloration in the filament to the right is from some slight contamination.

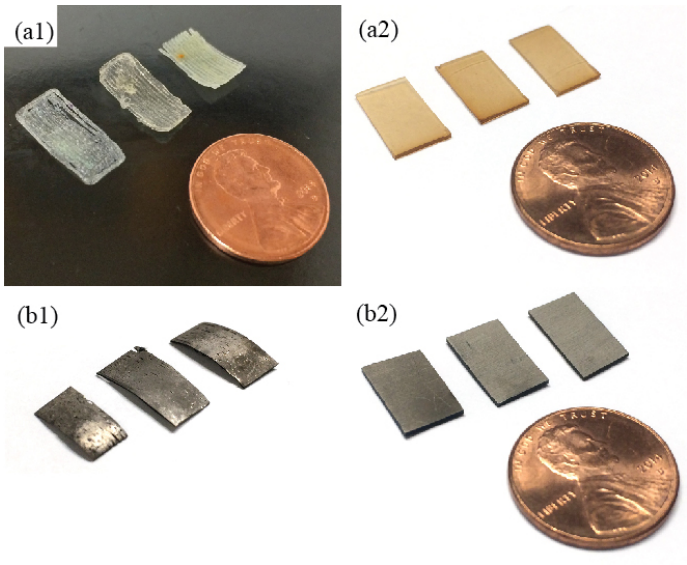

Figure 7. Printed and conventional samples: (a1) Printed membranes of Nafion precursor. (b1) IPMCs made from the printed membranes via the electroless plating process. (a2) Membranes of Nafion cut from commercially obtained 0.5 mm thick stock. (b2) IPMCs made from the commercially obtained Nafion membranes via the electroless plating process.

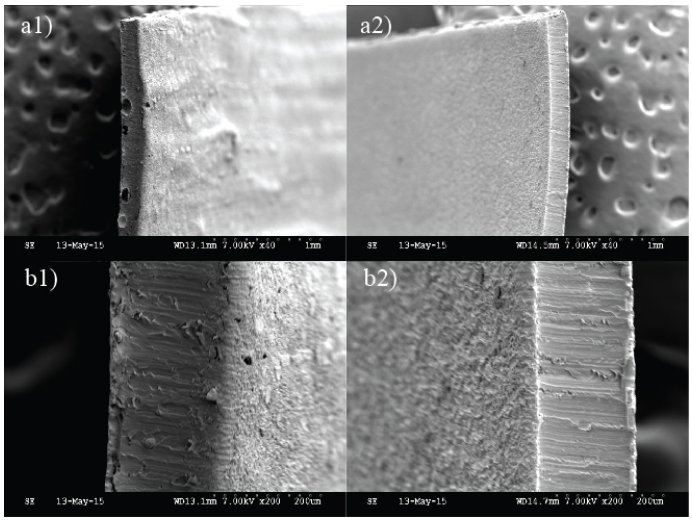

Figure 8. Scanning electron microscope (SEM) micrographs of a printed and conventional IPMC:(a1) Printed IPMC at x40 mag. (a2) Conventional IPMC at x40 mag. (b1) Printed IPMC at x200 mag. (b2) Conventional IPMC at x200 mag.

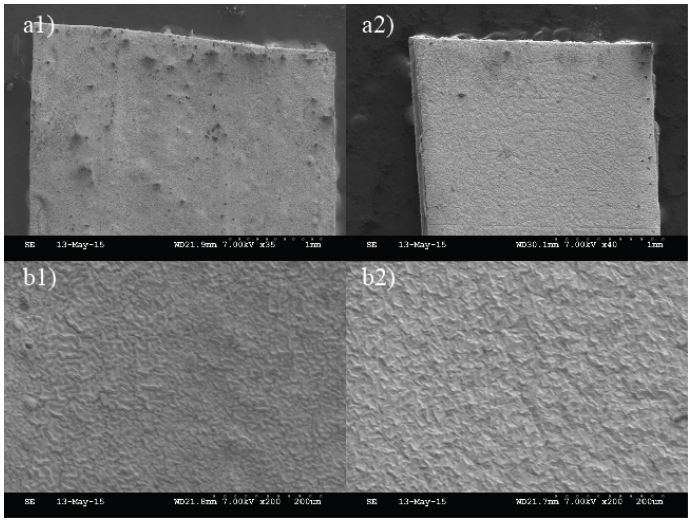

Figure 9. Scanning electron microscope (SEM) micrographs of the electrode surfaces of printed and conventional IPMCs: (a1) Printed IPMC electrode surface at x40 mag. (a2) Conventional IPMC electrode surface at x40 mag. (b1) Printed IPMC electrode surface at x200 mag. (b2) Conventional IPMC electrode surface at x200 mag.

mercially obtained sheets and a grain direction is visible in the printed membranes.

Scanning electron microscope (SEM) micrographs of a printed IPMC sample compared to a conventional IPMC sample are shown in Fig. 8. Images of the electrode surfaces of the same printed and conventional IPMCs are also compared in Fig. 9. The composition of the printed and conventional IPMCs appear similar from the cross-sections of the IPMCs shown in Fig. 8. Notable differences are that the printed IPMC is more uneven on one side (the side not against the build stage during the printing process) and porosity is present in the printed IPMC. The porosity could be a result of how multiple traces fuse together to form a layer in the 3D printing process, producing an uneven surface. The porosity could also be caused by gas pockets from the filament extrusion and printing processes. These issues can be mitigated with better tuning of the extrusion process as well as tuning and optimization of the 3D printing step.

Likewise, the electrode surface of the printed and conventional IPMCs are displayed in Fig. 9, where the resulting images show similarities. For instance, both electrode surfaces exhibit a “mud-cracked” texture caused by drying the IPMCs [36]. However, one notable difference is that the texture of the printed

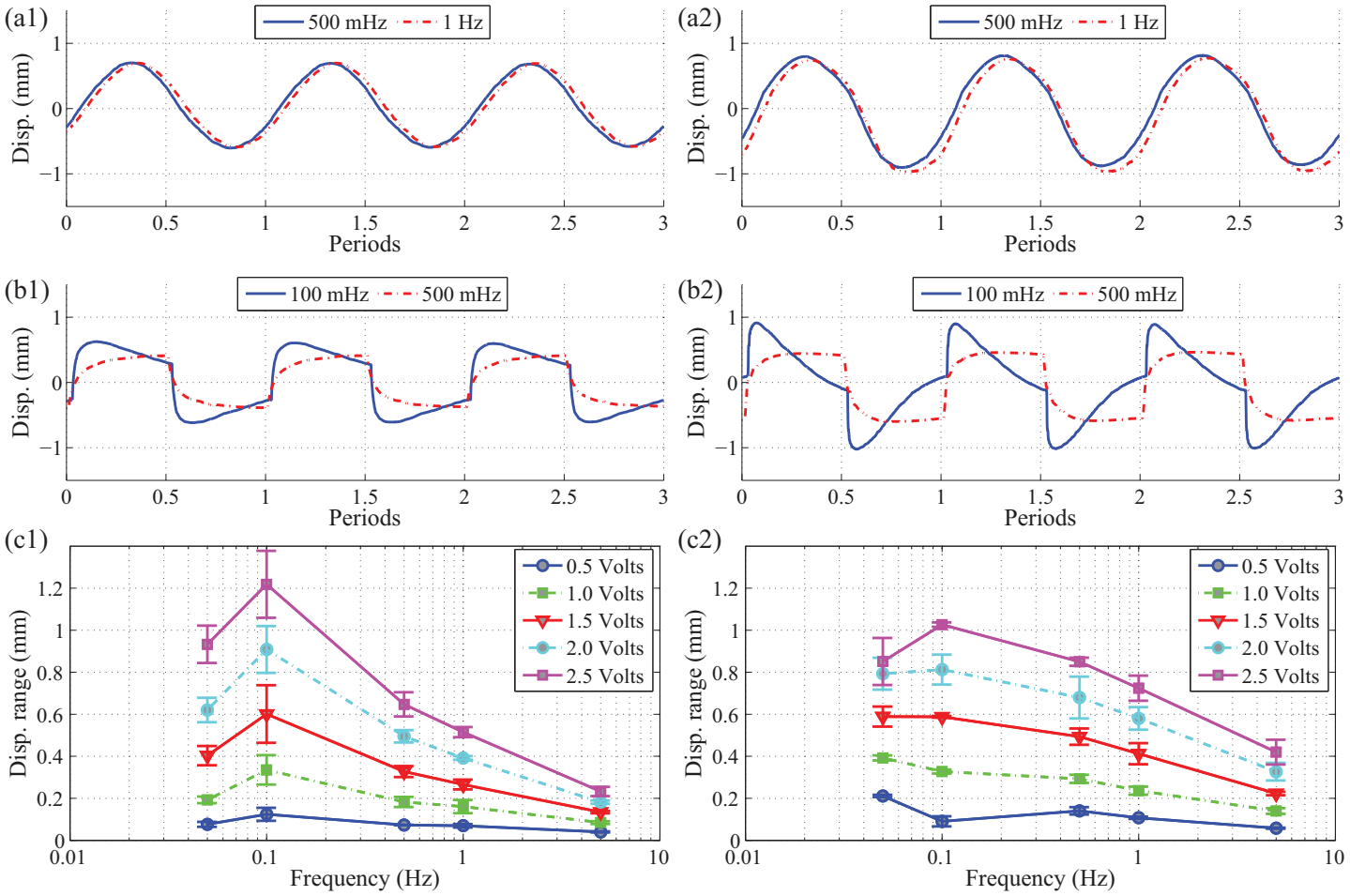

Figure 10. Actuation results: (a1) Time response of a 3D printed IPMC to 500 mHz and 1 Hz sine wave inputs. (a2) Time response of a conventional IPMC to 500 mHz and 1 Hz sine wave inputs. (b1) Time response of a 3D printed IPMC to 100 mHz and 500 mHz square wave inputs. (b2) Time response of a conventional IPMC to 100 mHz and 500 mHz square wave inputs. (c1) Range of response of a 3D printed IPMC to different sinusoidal inputs. Error bar range is six standard deviations. (c2) Range of response of a conventional IPMC to different sinusoidal inputs. Error bar range is six standard deviations.

electrode surface exhibits circular features that the texture of the conventional electrode surface does not exhibit. These features could also be a result of gas inside the printed membrane during the 3D printing process. Thus it is believed that tuning and optimization of the 3D printing step is highly critical. Future work will consider processing tuning.

3.3 Actuation Performance

To test the actuation performance of the 3D printed IPMCs and to compare them to those of conventional IPMCs, the same IPMCs shown in Fig. 8 were driven with periodic signals while their tip displacements was being recorded. The measured time responses and photographs of the actuation performance are shown in Fig. 10 and 11, respectively. The IPMCs were driven in distilled water. Gold plated neodymium magnets were used to fixture the IPMCs (as shown in Fig. 11) and to make electrical contact with the fixtured regions of the electrodes. A Keyence LK-031 laser displacement sensor was used to measure the deflection of the tip of the IPMC actuator. A National Instruments Lab-PC+ data acquisition system was used to log the input and

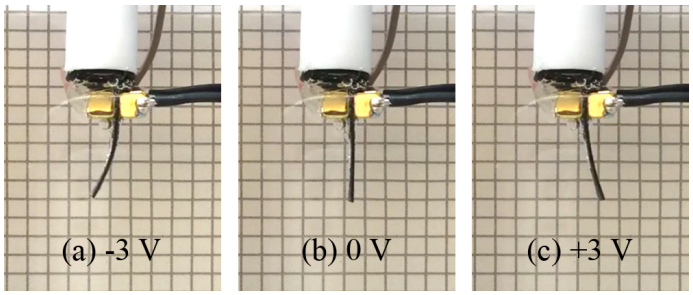

Figure 11. Actuation results: (a) The deflection of the printed IPMC to a -3 volt input. (b) The equilibrium position of the printed IPMC given zero input. (c) The deflection of the printed IPMC to a 3 volt input.

sensor signals. A custom built voltage/current amplifier was used to drive the IPMC sample. The response was obtained for both printed and conventional IPMCs to sinusoidal and square wave input signals at frequencies of 50 mHz, 100 mHz, 500 mHz, 1 Hz, and 5 Hz and voltage amplitude varied between 0.5 to 3 volts in 0.5-volt increments for each of these frequencies. Figure 11(a) shows the deflection of the printed IPMC to a -3 volt

input, Fig. 11(b) shows the equilibrium position of the printed IPMC given zero input, and Fig. 11(c) shows the deflection of the printed IPMC to a +3 volt input. Figure 10(a1) and (a2) show the time response of the printed and conventional IPMCs, respectively, to 500 mHz and 1 Hz sinusoidal inputs. Figure 10(b1) and (b2) show the time response of the printed and conventional IPMCs respectively to 100 mHz and 500 mHz square wave inputs. Figure 10(c1) and (c2) show the max range of the response of the printed and conventional IPMCs respectively, over the frequency range for each tested voltage. The error bars shown in Fig. 10(c1) and (c2) are based on a six-sigma confidence interval for ease of viewing. Overall, these results show that the performance of the 3D printed IPMCs are very comparable to that of conventionally manufactured IPMCs. The printed IPMC shows a somewhat slower response and less dramatic back relaxation compared to the conventional IPMC. This leads to a superior response at lower frequencies and a more diminished response at higher frequencies, for a sinusoidal input. However, this is well within the range of behavior of conventionally manufactured IPMCs in general.

4 Conclusions and Future Work

This paper has presented a fused filament additive manufacturing (3D printing) technique for IPMC materials to create soft active 3D structures. A custom-designed 3D printer was described that utilizes custom-extruded IPMC filament made from raw precursor material. For the first time, the unique actuation and sensing properties of ionic polymer-metal composites (IPMCs) was exploited and directly incorporated into the structural design and experimental results were presented to demonstrate a functioning IPMC actuator fabricated via the 3D printing process. The proposed 3D manufacturing technique can be used to create sub-millimeter scale cilia-like actuators and sensors to macro-scale soft robotic systems. Future work will consider the possibility of eliminating the step of fabricating precursor filament, before printing and incorporating post printing processes such as the activation process and plating process into the printer design. Additionally, the tuning and optimization of the 3D printing process will also be explored.

5 Acknowledgments

Authors acknowledge financial support, in part, from the Office of Naval Research, grant number N00014-13-1-0274. Authors also thank Prof. Kwang J. Kim and Dr. Viljar Palmre for their time during technical discussions.

REFERENCES

[1] Jones, R., Haufe, P., Sells, E., Iravani, P., Olliver, V., Palmer, C., and Bowyer, A., 2011. "RepRap the replicating rapid prototyper". *Robotica*, ***29***(1), pp. 177 – 191.

[2] Schubert, C., van Langeveld, M. C., and Donoso, L. A., 2013. "Innovations in 3D printing: a 3D overview from optics to organs". *British Journal of Ophthalmology*.

[3] Shahinpoor, M., and Kim, K. J., 2001. "Ionic polymer-metal composites: I. fundamentals". *Smart materials and structures*, ***10***(4), p. 819.

[4] Shahinpoor, M., Kim, K. J., and Mojarrad, M., 2007. *Artificial Muscles: Applications of Advanced Polymeric Nano-Composites*. Springer, London.

[5] Tiwari, R., and Garcia, E., 2011. "The state of understanding of ionic polymer metal composite architecture: a review". *Smart Materials and Structures*, ***20***(8), p. 083001.

[6] Guo, S., Fukuda, T., Kosuge, K., Arai, F., Oguro, K., and Negoro, M., 1994. "Micro catheter system with active guide wire-structure, experimental results and characteristic evaluation of active guide wire catheter using icpf actuator". In Proceedings International Symposium on Micro Machine and Human Science (MMHS), pp. 191–197.

[7] Fang, B.-K., Ju, M.-S., and Lin, C.-C. K., 2007. "A new approach to develop ionic polymer–metal composites (IPMC) actuator: Fabrication and control for active catheter systems". *Sensors and Actuators A: Physical*, ***137***(2), pp. 321–329.

[8] Fang, B.-K., Lin, C.-C. K., and Ju, M.-S., 2010. "Development of sensing/actuating ionic polymer–metal composite (IPMC) for active guide-wire system". *Sensors and Actuators A: Physical*, ***158***(1), pp. 1–9.

[9] Shuxiang, G., and Kinji, A., 2004. "A new type of micropump driven by a low electric voltage". *Acta Mechanica Sinica*, ***20***(2), pp. 146–151.

[10] Ramírez-García, S., and Diamond, D., 2007. "Biomimetic, low power pumps based on soft actuators". *Sensors and Actuators A: Physical*, ***135***(1), pp. 229–235.

[11] Nguyen, T. T., Goo, N. S., Nguyen, V. K., Yoo, Y., and Park, S., 2008. "Design, fabrication, and experimental characterization of a flap valve IPMC micropump with a flexibly supported diaphragm". *Sensors and Actuators A: Physical*, ***141***(2), pp. 640–648.

[12] Lee, S., and Kim, K. J., 2006. "Design of IPMC actuator-driven valve-less micropump and its flow rate estimation at low reynolds numbers". *Smart Materials and Structures*, ***15***(4), p. 1103.

[13] Guo, S., Fukuda, T., and Asaka, K., 2003. "A new type of fish-like underwater microrobot". *Mechatronics*, ***8***(1), pp. 136–141.

[14] Aureli, M., Kopman, V., and Porfiri, M., 2010. "Free-locomotion of underwater vehicles actuated by ionic polymer metal composites". *Mechatronics, IEEE/ASME Transactions on*, ***15***(4), pp. 603–614.

[15] Hubbard, J. J., Fleming, M., Palmre, V., Pugal, D., Kim, K. J., and Leang, K. K., 2014. "Monolithic IPMC fins for propulsion and maneuvering in bio-inspired underwater robotics". *Journal of Oceanic Engineering*, ***39***(3), pp. 540 – 551.

[16] Lee, S. J., Han, M. J., Kim, S. J., Jho, J. Y., Lee, H. Y., and Kim, Y. H., 2006. "A new fabrication method for ipmc actuators and application to artificial fingers". *Smart Materials and Structures*, ***15***(5), p. 1217.

[17] Kim, K. J., and Shahinpoor, M., 2002. "A novel method of manufacturing three-dimensional ionic polymer–metal

composites (ipmcs) biomimetic sensors, actuators and artificial muscles". *Polymer,* ***43***(3), pp. 797–802.

[18] Tondu, B., Ippolito, S., Guiochet, J., and Daidie, A., 2005. "A seven-degrees-of-freedom robot-arm driven by pneumatic artificial muscles for humanoid robots". *The International Journal of Robotics Research,* ***24***(4), pp. 257–274.

[19] Grzesiak, A., Becker, R., and Verl, A., 2011. "The bionic handling assistant: A success story of additive manufacturing". *Assembly Automation,* ***31***(4), pp. 329–333.

[20] Vogt, D., Park, Y.-L., and Wood, R., 2013. "Design and characterization of a soft multi-axis force sensor using embedded microfluidic channels". *Sensors Journal,* ***13***(10), pp. 4056–4064.

[21] Hannan, M. W., and Walker, I. D., 2003. "Kinematics and the implementation of an elephant's trunk manipulator and other continuum style robots". *Journal of Robotic Systems,* ***20***(2), pp. 45–63.

[22] Umedachi, T., Vikas, V., and Trimmer, B. A., 2013. "Highly deformable 3-D printed soft robot generating inching and crawling locomotions with variable friction legs". In Proceedings Intelligent Robots and Systems (IROS), IEEE, pp. 4590–4595.

[23] Cho, K.-J., Koh, J.-S., Kim, S., Chu, W.-S., Hong, Y., and Ahn, S.-H., 2009. "Review of manufacturing processes for soft biomimetic robots". *International Journal of Precision Engineering and Manufacturing,* ***10***(3), pp. 171–181.

[24] Cheng, N., Ishigami, G., Hawthorne, S., Chen, H., Hansen, M., Telleria, M., Playter, R., and Iagnemma, K., 2010. "Design and analysis of a soft mobile robot composed of multiple thermally activated joints driven by a single actuator". In Proceedings Robotics and Automation (ICRA), IEEE, pp. 5207–5212.

[25] Koh, J.-S., Lee, D.-Y., and Cho, K.-J., 2012. "Design of the shape memory alloy coil spring actuator for the soft deformable wheel robot". In Proceedings Ubiquitous Robots and Ambient Intelligence (URAI), 2012 9th International Conference on, pp. 641–642.

[26] Ming, A., Hashimoto, K., Zhao, W., and Shimojo, M., 2013. "Fundamental analysis for design and control of soft fish robots using piezoelectric fiber composite". In Proceedings Mechatronics and Automation (ICMA), pp. 219–224.

[27] Malone, E., and Lipson, H., 2006. "Freeform fabrication of ionomeric polymer-metal composite actuators". *Rapid Prototyping Journal,* ***12***(5), pp. 244–253.

[28] Malone, E., and Lipson, H., 2008. "Multi-material freeform fabrication of active systems". In Proceedings 9th Biennial Conference on Engineering Systems Design and Analysis, ASME, pp. 345–353.

[29] Mauritz, K. A., and Moore, R. B., 2004. "State of understanding of nafion". *Chemical reviews,* ***104***(10), pp. 4535–4586.

[30] Moore, R. B., Cable, K. M., and Croley, T. L., 1992. "Barriers to flow in semicrystalline ionomers. A procedure for preparing melt-processed perfluorosulfonate ionomer films and membranes". *Journal of Membrane Science,* ***75***(1), pp. 7–14.

[31] Oguro, K., 2000. Preparation procedure ion-exchange polymer metal composites (IPMC) membranes. On the WWW, feb. URL `http://ndeaa.jpl.nasa.gov/`.

[32] Kim, K. J., and Shahinpoor, M., 2003. "Ionic polymer–metal composites: II. manufacturing techniques". *Smart Materials and Structures,* ***12***(1), p. 65.

[33] Bhandari, B., Lee, G.-Y., and Ahn, S.-H., 2012. "A review on ipmc material as actuators and sensors: fabrications, characteristics and applications". *International journal of precision engineering and manufacturing,* ***13***(1), pp. 141–163.

[34] DuPont Fluoroproducts, 2002. Chemical treatment of nafion PFSA resins R-1100 and R-1000, nov. URL `www.ion-power.com`.

[35] Elliott, J. A., James, P. J., McMaster, T. J., Newton, J. M., Elliott, A., Hanna, S., and Miles, M. J., 2001. "Hydrolysis of the nafion precursor studied by x-ray scattering and in-situ atomic force microscopy". *e-Polymers,* ***1***(1), pp. 210–220.

[36] Lu, J., Kim, S.-G., Lee, S., and Oh, I.-K., 2008. "A biomimetic actuator based on an ionic networking membrane of poly (styrene-alt-maleimide)-incorporated poly (vinylidene fluoride)". *Advanced Functional Materials,* ***18***(8), pp. 1290–1298.